tRNA-linked molecular beacons for imaging mRNAs in the cytoplasm of living cells

Musa M. Mhlanga[1], Diana Y. Vargas, Cindy W. Fung, Fred Russell Kramer[1] and Sanjay Tyagi*

Department of Molecular Genetics, Public Health Research Institute, 225 Warren Street, Newark, NJ 07103, USA and [1]Department of Cell Biology, New York University School of Medicine, New York, NY 10016, USA

ABSTRACT

When oligonucleotide probes are microinjected into cells to image the distribution of RNAs, they are rapidly sequestered into the nucleus. As a result, it is difficult to detect mRNAs in the cytoplasm of living cells. We were able to overcome this process by attaching tRNA transcripts to the probes. We show that when fluorescently labeled tRNAs, tRNAs with extensions at their 5′ end, or chimeric molecules in which a molecular beacon possessing a 2′-O-methyl-ribonucleotide backbone is linked to a tRNA, are injected into the nucleus of HeLa cells, they are exported into the cytoplasm. When these constructs are introduced into the cytoplasm, they remain cytoplasmic. These constructs allow the distribution of both the general mRNA population and specific mRNAs to be imaged in living cells. This strategy should also be useful for enhancing the efficacy of antisense oligonucleotides by keeping them in the cytoplasm. Our observations show that the fidelity of the tRNA export system is relaxed for unnatural tRNA variants when they are introduced into the nucleus in large amounts.

INTRODUCTION

Genetically encoded fluorescent tags have been instrumental in studies of the distribution and dynamics of specific proteins in live cells. The ability to label particular RNAs in living cells would similarly be useful in studies of the intracellular distribution, trafficking and localization of specific RNAs. The significance of localization of mRNAs in subcellular regions has been established in oocytes, in early embryos and in a variety of somatic cells (1). Elucidation of the mechanisms and pathways that lead to RNA localization would benefit if a general method to visualize specific RNAs in living cells was available. Such methods would also aid in studies of temporal changes in the expression of specific genes.

The quest to visualize specific endogenous RNAs in living cells began immediately after the development of fluorogenic hybridization probes (2–5). One of the earliest methods utilizes a pair of complementary oligonucleotides, in which one of the oligonucleotides serves as a probe for a single-stranded RNA target. The 5′ end of one oligonucleotide is labeled with a donor fluorophore and the 3′ end of the complementary oligonucleotide is labeled with an acceptor fluorophore, such that when the two oligonucleotides are annealed to each other, fluorescence resonance energy transfer (FRET) occurs. Since small complementary oligonucleotides bind to each other in a dynamic equilibrium, target strands compete for binding to the probe, causing the separation of the labeled oligonucleotides and the restoration of the fluorescence of the donor (4). Utilizing this method, Sixou *et al*. (6) were able to detect synthetic oligonucleotides that were injected into cells. A second method for homogeneous hybridization utilizes a pair of oligonucleotide probes that are labeled at their respective 5′ and 3′ ends, and that can bind to adjacent sites on a target strand. The presence of the target enables the donor and acceptor moieties to become sufficiently close to each other, causing FRET to occur (2,3). Tsuji *et al*. (7) used this approach to image the distribution of an mRNA that was expressed from a transfected plasmid. We have developed a third approach, in which internally quenched hairpin-shaped oligonucleotide probes, called molecular beacons, are used. Molecular beacons possess complementary sequences on either end of a probe sequence, enabling the molecule to assume a hairpin configuration in which a fluorophore and quencher are held in close proximity. The formation of the probe–target hybrid disrupts the hairpin stem, removing the fluorophore from the vicinity of the quencher, restoring the probe's fluorescence and revealing the presence of the target (5). A number of different RNAs have since been detected in living cells utilizing this approach (8–10).

An ideal probe should itself be distributed homogenously within the cell and produce signals only in those regions where the target appears. However, it has been reported that microinjected oligonucleotides, such as antisense agents, are rapidly transported from the cytoplasm into the nucleus (11,12). When oligonucleotides are internalized by the cells through endocytosis, they are initially localized in the cytoplasm because they reside within the endosomes. However, they migrate to the nucleus after their escape from the membranous compartments (13,14). When the oligonucleotides are introduced into the cells with the help of pore-forming agents, such as streptolysin-O, the bulk of the oligonucleotides are found in the nucleus (15). The same phenomenon is encountered when the oligonucleotides are used as probes and are microinjected into cells (6,7). We have observed that molecular beacons are similarly sequestered in the nucleus after their microinjection into the cytoplasm, and this sequestration is so rapid and extensive that the probes are not able to hybridize to their cytoplasmic target mRNAs before they are shunted to the nucleus (16). In contrast to these observations, Santangelo *et al*. (17) and Nitin *et al*. (18) report that molecular beacons delivered into the cells with the help of streptolysin-O and cell penetrating peptides, reside within the cytoplasm.

There are two possible approaches that may be employed to overcome the problem of nuclear sequestration of molecular beacons subsequent to their delivery by microinjection. A non-karyophilic protein that cannot traverse nuclear pores can be linked to the probes to prevent their entry into the nucleus (7,16), or it may be possible to exploit the cell's own endogenous nucleo-cytoplasmic transport system in such a manner that the probe is identified as cargo to be exported out of the nucleus. For example, we could tag molecular beacons with a signal motif that would confer a cytoplasmic fate upon the probe. Among suitable motifs are nuclear export signals commonly found in cytoplasmic proteins (19) and the constitutive transport element found in the genomic RNA of the Mason–Pfizer monkey virus (20). In the present study, we exploited the natural export mechanism of tRNAs as a means of keeping molecular beacons within the cytoplasm. tRNAs are produced in the nucleus, but function in the cytoplasm. They are the most abundant form of RNA in the cell. Their export machinery should therefore be able to transport a large amount of probe out of the nucleus. More than 40 species of tRNAs exist in mammalian cells and they are all exported from the nucleus using the same pathway (21). Thus, the tRNA export system may be sufficiently permissive to allow the export of heterologous cargo. Reasoning similarly, Kuwabara *et al*. (22) have shown that the activity of a ribozyme can be improved by expressing it as part of a joint transcript containing a tRNA sequence, and by using a tRNA promoter.

In this work, we have studied the export of fluorescently labeled synthetic transcripts of human valine tRNA in HeLa and Chinese hamster ovary (CHO) cells. In order to determine if tRNA transcripts can serve as carriers for the export of molecular beacons, we studied the export of RNA transcripts that had a molecular beacon sequence at one end and a tRNA sequence at the other end. We then prepared chimeric molecules in which molecular beacons with a 2′-*O*-methyl-ribonucleotide backbone were linked to tRNA, either chemically or via engineered sticky ends. With these constructs, we showed that the linkage of a molecular beacon to a tRNA

transcript prevents the nuclear sequestration of the probe and enables the imaging of specific cytoplasmic mRNAs in living cells.

MATERIALS AND METHODS

Molecular beacons

Molecular beacons were synthesized on an Applied Biosystems 394 DNA synthesizer (Foster City, CA) using 2′-*O*-methylribonucleotide-β-cyanoethyl phosphoramidites. The sequences of the molecular beacons and the location of different labels are indicated in Table 1. For the synthesis of molecular beacons that had a quencher at their 3′ end, a controlled-pore glass column containing Black Hole Quencher 2 (BHQ2) was used, whereas for molecular beacons possessing an internal quencher, a thymidine-BHQ2 phosphoramidite or a thymidine-dabcyl phosphoramidite was used. In order to attach the fluorophore, the last residue added during automated synthesis possessed a 5′-terminal sulf-hydryl group protected by a trityl moiety. Each oligonucleotide was purified by high-pressure liquid chromatography (HPLC) through a C-18 reverse-phase column, while the trityl moiety was still attached. An iodoacetamide derivative of tetramethylrhodamine (TMR) or Texas red was then coupled to the 5′-sulfhydryl group. DNA synthesis reagents were obtained from Glen Research (Sterling, VA) and Biosearch Technologies (Novato, CA), and activated fluorophores were obtained from Molecular Probes (Eugene, OR). Completed oligonucleotides were purified by using HPLC, and their signal-to-background ratio was determined as described previously (23). A detailed protocol for molecular beacon synthesis is available at http://www.molecular-beacons.org.

RNA transcripts

RNAs were synthesized by *in vitro* transcription using bacteriophage T7 RNA polymerase and synthetic DNA templates that were generated in a series of polymerase chain reactions using appropriately tailed primers (Table 1). First, primer tRNA Forward and primer tRNA Reverse were annealed to each other, and their 3′ ends were then extended to produce a DNA that corresponded to the sequence of human valine tRNA (22). Using this DNA as a template and a combination of different primers in separate polymerase chain reactions, we prepared DNA templates possessing a bacteriophage T7 promoter for each of the RNAs used in this study. Primer T7 tRNA Forward and primer tRNA Reverse Short were used to generate the template for transcripts of tRNA; primer T7 poly(T) tRNA Forward and primer tRNA Reverse Short were used to generate the template for MB poly(U)-tRNA; and primer T7 tRNA Forward and primer T7 tRNA Sticky End Reverse were used to generate the template for RNA tRNA-Sticky End. Standard T7 RNA polymerase transcription reactions (Promega, Madison, WI), using 0.5 mM of each ribonucleotide triphosphate, were performed for RNA synthesis. In order to produce internally labeled fluorescent RNAs, 90% of the UTP in the transcription mixture was replaced with TMR-labeled UTP (Molecular Probes). All of the RNAs were purified by electrophoresis through 8% polyacrylamide gels under denaturing conditions, followed by elution from the gel and precipitation.

Table 1. Sequences of molecular beacons, transcripts of tRNA and its variants, and primers

Construct	Sequence
Molecular beacons	
MB Analogue 1	TMR-<u>GCCGGGC</u>GAAGAAUGAAAAC<u>GGC</u>
MB Analogue 2	TMR(or Texas red)-<u>CAAGG</u>CTTCGTC<u>CC</u>ACAAACAC<u>CCTTGG</u>TCGCTGCGGGCGGG
MB poly(U)-linker-tRNA	TMR-<u>GGACC</u>UUUUUUUUUUUUUUUUUUUUUUU<u>GGUCC</u>-(dT-dabcyl)-TTTT-linker-GUUUCCGUAGUGUAGUGG UUAUCACGUUCGCCUAACACGCGAAAGGUCCCCGGUUCGAAACCGGGCGGAAACACCA
MB β-actin-38-61	TMR(or Texas red)-<u>CCACGG</u>AGUAACGCGGUCAGUCAGG<u>UGG</u>-BHQ2-**GUCGCUGCGGGCGGG**
MB β-actin-66-83	TMR(or Texas red)-<u>CAAU</u>AUCAUCAUCCAUGGC<u>AUUG</u>-BHQ2-**GUCGCUGCGGGCGGG**
MB β-actin-240-262	TMR(or Texas red)-<u>CGAC</u>AGGAUACCUCUUUUGCUCUGG<u>GUCG</u>-BHQ2-**GUCGCUGCGGGCGGG**
RNA transcripts	
tRNA[val]	GUUUCCGUAGUGUAGUGGUUAUCACGUUCGCCUAACACGCGAAAGGUCCCCGGUUCGAAACCG GGCGGAAACACCA
MB poly(U)-tRNA	<u>GGACC</u>UUUUUUUUUUUUUUUUUUUUUU<u>GGUCC</u>GUUUCCGUAGUGUAGUGGUUAUCACGUUCGCCUAAC ACGCGAAAGGUCCCCGGUUCGAAACC<u>GGGCGG</u>AAACACCA
tRNA-Sticky End	GUUUCCGUAGUGUAGUGGUUAUCACGUUCGCCUAACACGCGAAAGGUCCCCGGUUCGAAACCGGGCGGAA ACACCA**CCCGCCCGCAGCGAC**
Primers	
tRNA Forward	GTTTCCGTAGTGTAGTGGTTATCACGTTCGCCTAACACGCGAAAGGTC
tRNA Reverse	TGGTGTTTCCGCCCGGTTTCGAACCGGGGACCTTTCGCGTGTTAGGCG
tRNA Reverse Short	TGGTGTTTCCGCCCGGTTTC
T7 tRNA Forward	GCATAATACGACTCACTATAGGGAGAGTTTCCGTAGTGTAGTGG
T7 poly(T) tRNA Forward	GCATAATACGACTCACTATAGGGAGAGGACCTTTTTTTTTTTTTTTTTTTTTTTGGTCCGTTTCCGTAGTGTAGTG
T7 tRNA Sticky End Reverse	GTCGCTGCGGGCGGGTGGTGTTTCCGCCCGGTTTC

The underlined nucleotides identify sequences that form hairpin stems and bold nucleotides identify sticky ends. The structure of the linker in MB poly(U)-linker-tRNA is depicted in Figure 4A. The numbers in the names of β-actin mRNA-specific molecular beacons refer to positions in the β-actin mRNA sequence (accession number L08165). The sequence of human tRNA valine corresponds to the sequence reported by Kuwabara *et al.* (22). All sequences are listed from their 5′ end to their 3′ end. All molecular beacons have a 2′-*O*-methylribonucleotide backbone, except MB poly(U)-linker-tRNA, in which the molecular beacon portion of the construct possesses a 2′-*O*-methylribonucleotide backbone and the tRNA portion of the construct possesses a natural ribonucleotide backbone.

Labeling tRNAs at their 5′ ends and linking them to molecular beacons

In order to label RNAs at their 5′ end with a fluorophore, we exploited the capacity of T7 RNA polymerase to incorporate guanosine monophosphate (GMP) and its derivatives at the first position (5′ end) of the RNA product (24). We synthesized a TMR derivative of GMP by coupling 5′-thio-guanosine monophosphate (5′-thio-GMP) (Biolog, Bremen, Germany) to TMR iodoacetamide. The resulting TMR-S-GMP was purified using HPLC. In order to synthesize terminally labeled RNAs, 90% of the GTP in the transcription mixture was replaced with TMR-S-GMP. This derivative of GMP was efficiently incorporated into RNA transcripts by T7 RNA polymerase.

In order to covalently link tRNA to molecular beacons, we introduced a sulfhydryl group at the 5′ end of the tRNA and a primary amino group at the 3′ end of the molecular beacon. These groups were then linked to each other utilizing mal-sac-HNSA (Bachem, King of Prussia, PA), a heterobifunctional agent that possesses a maleimide moiety for coupling to a sulfhydryl group and a succinimidyl ester moiety for coupling to a primary amino group (25). Molecular beacon-tRNA adduct MB poly(U)-linker-tRNA was produced by first coupling mal-sac-HNSA to the 3′-amino group of molecular beacon MB poly(U). For this reaction, 10 mg mal-sac-HNSA and 0.5 mg molecular beacon MB-poly(U) were mixed together in 500 μl 0.1 M sodium phosphate buffer (pH 7.4). After a 1 h incubation at 25°C, when the color of the reaction mixture turns yellow, which is indicative of successful coupling to the amino group, the excess mal-sac-HNSA and side products were removed by gel filtration through a NAP-5 Sephadex column (Amersham, Uppsala, Sweden). In parallel, we synthesized tRNA with a 5′-sulfhydryl group. For this

purpose, we replaced 90% of the GTP in the *in vitro* transcription reaction mixture with 5′-thio-GMP. The excess nucleotides were removed by filtration using a NAP-5 column. Both columns were equilibrated and eluted with 0.1 M sodium phosphate buffer (pH 6.0). The 5′-thio-tRNA and the succinimidyl-MB poly(U) thus produced were mixed together and the reaction was incubated for 16 h. The phosphate was removed from the mixture by another passage through a NAP-5 column and the nucleic acids were precipitated. The linked product was purified by denaturing polyacrylamide gel electrophoresis.

In order to link tRNA to molecular beacons via engineered sticky ends, the transcription reaction that was carried out to produce tRNA with sticky ends was terminated by phenol extraction and then an equimolar amount of molecular beacon with complementary sticky ends was added. After a 1 h incubation at 25°C, the annealed nucleic acids were purified by non-denaturing polyacrylamide gel electrophoresis, followed by elution and precipitation.

Real-time hybridization reactions (125 μl) were incubated at 37°C in a spectrofluorometer (Photon Technology International, Lawrenceville, NJ). The reaction mixtures contained 8 nM of each molecular beacon (either free in solution or linked to a tRNA-transcript via its cohesive end), 7.5 mM MgCl$_2$ and 20 mM Tris–HCl (pH 8.0). The hybridization was initiated by the addition of a 4-fold molar excess of β-actin mRNA (2 μl of a 2 μM solution) after recording the baseline fluorescence for 1 min. Chicken β-actin mRNA was synthesized as described previously (16).

Microinjection, transfection and live cell imaging

HeLa cells were cultured in Dulbecco's modification of Eagle's medium (Mediatech, Herndon, VA) supplemented

with 10% fetal bovine serum, and CHO cells were cultured in the alpha modification of the same medium. Conditions for culturing chicken embryonic fibroblasts have been described previously (16). For live cell imaging, we used black T4 culture dishes (Bioptechs, Butler, PA) possessing a 0.17 mm cover glass with a coating of conductive material at their bottom to permit controlled heating. These dishes were coated with gelatin before plating the cells. The temperature of the T4 culture dishes and the microscope objective was maintained at 37°C using two Bioptech controllers. During microinjection and imaging, the cells were maintained in Leibovitz's L-15 media (Invitrogen, Carlsbad, CA) that lacked the dye phenol red, and was thus optically more transmissive and had less autofluorescence.

Microinjections were performed using a Femtojet microinjection apparatus (Eppendorf, Hamburg, Germany). The concentrations of the different constructs injected into HeLa cells were MB Analogue 1, 0.5 µM; tRNA, 0.5 µM; MB poly(U)-tRNA, 0.5 µM; and MB poly(U)-linker-tRNA, 1.0 µM. In order to prepare dextran for co-injection, amino dextran (Molecular Probes) was labeled with fluorescein using fluorescein succinimidyl ester (Molecular Probes), and unreacted fluorophore was removed by gel filtration. The amount of dextran to be included in the injection mixtures was optimized so that its fluorescence intensity in the nucleus would be similar to the fluorescence intensity stemming from the construct that was co-injected. The mixture that was injected into CHO cells to determine the intracellular distribution of MB Analogue 2 contained 0.4 µM of TMR-labeled MB Analogue 2 annealed to tRNA-Sticky End and 0.4 µM Texas red-labeled MB Analogue 2. The mixture injected into chicken embryonic fibroblasts to image β-actin mRNA contained 0.5 µM each of three β-actin mRNA-specific molecular beacons labeled with Texas red and linked to tRNA and each of three β-actin mRNA-specific molecular beacons labeled with TMA but not linked to tRNA (Table 1). All microinjected reagents were dissolved in water.

In order to introduce MB Analogue 1 into CHO cells via transfection, the cells were cultured in T4 culture dishes to 70% confluency and washed with serum-free Opti-MEM1 (Invitrogen). The transfection reagent oligofectamine (Invitrogen) was incubated for 5 min in serum-free medium (1 µl reagent added to 9 µl Opti-MEM1) before mixing with MB Analogue 1 (1 ng/µl in Opti-MEM1). The oligonucleotide and the transfection reagent were incubated for 20 min at 25°C to form complexes between them. After diluting these complexes with 200 µl serum-free medium, they were added to the cells. The cells were incubated for 3 h in the presence of these complexes. Finally, the cells were washed with Leibovitz's media containing serum, and then imaged.

An Axiovert 200M inverted fluorescence microscope (Zeiss, Oberkochen, Germany), equipped with a 40× or 100× objective and a Photometrics Coolsnap HQ camera (Roper Scientific, Trenton, NJ) cooled to −30°C, was used to obtain the images. The excitation filters, dichroic mirrors and emission filters used for different fluorophores were, respectively: 475AF20, 500DRLP and 530DF30 for fluorescein; 546DF10, 555DRLP and 580DF30 for TMR; and 590DF10, 610DRLP and 630DF30 for Texas red. All of the filters were obtained from Omega Optical (Brattleboro, VT). The filter sets were so specific that no detectable cross-talk occurred among the different channels. The images were acquired and analyzed using Openlab software (Improvision, Lexington, MA).

RESULTS

Sequestration of molecular beacons within nuclei

We recently demonstrated the ability of molecular beacons to report the distribution and trafficking of intracellular mRNAs by tracking the journey of *oskar* mRNA from a nurse cell to the posterior tip of a *Drosophila melanogaster* oocyte (10). Those probes (and all of the probes used in this study) were synthesized from 2′-O-methylribonucleotides, in order to protect them from cellular nucleases and to protect their hybrids with mRNA from ribonuclease H-mediated degradation in the cell. When *oskar* mRNA-specific molecular beacons are injected into the cytoplasm of nurse cells, they rapidly enter into the nucleus, where they hybridize to *oskar* mRNA. The hybrid is then exported to the cytoplasm of the nurse cells and travels onto the posterior cortex of the oocyte (10). However, when we attempted to image the distribution of cytoplasmic mRNAs in cells that are maintained in culture, we found that molecular beacons are rapidly sequestered into the nucleus and very little signal is observed in the cytoplasm.

In order to explore this phenomenon systematically, we prepared a molecular beacon analogue that did not possess a quencher and had a probe sequence that did not have any target within the cell (MB Analogue 1, Table 1). This analogue is fluorescent even when not bound to any nucleic acid. We introduced this oligonucleotide into the cytoplasm of a HeLa cell that was maintained at 37°C on the stage of a microscope. Images of this cell were obtained at different times after microinjection. Within several minutes after microinjection, the molecular beacon analogue became sequestered within the nucleus (Figure 1A). When the molecular beacons were injected directly into the nucleus they remained within the nucleus (Figure 1A). The overall fluorescence in the cell decreased over time, perhaps due to photobleaching or due to the leakage of the probes. In order to confirm that nuclear sequestration of molecular beacons is not a consequence of their delivery by microinjection, we introduced MB Analogue 1 into HeLa cells with the aid of the transfection reagent oligofectamine. In this mode of delivery too, the oligonucleotides became concentrated in the nucleus (Figure 1B).

It has been shown previously that the internalization of molecular beacons into nuclei occurs via an active transport mechanism, and once they are in the nucleus, they become even more concentrated in the nucleoli than in the rest of the nucleoplasm (16). We observed that nuclear sequestration occurs in a wide variety of cell types. It does not depend either on the nature of the molecular beacon backbone or on the identity of the attached fluorophores, as molecular beacons synthesized from deoxyribonucleotides, or those having peptide nucleic acid backbones, and molecular beacons labeled with a variety of different fluorophores, are all efficiently sequestered within the nucleus. Furthermore, nuclear sequestration also occurs when the probes have no stem. Similar observations have been made for antisense oligonucleotides that are introduced into cells to inhibit the expression of specific genes (11,12,26).
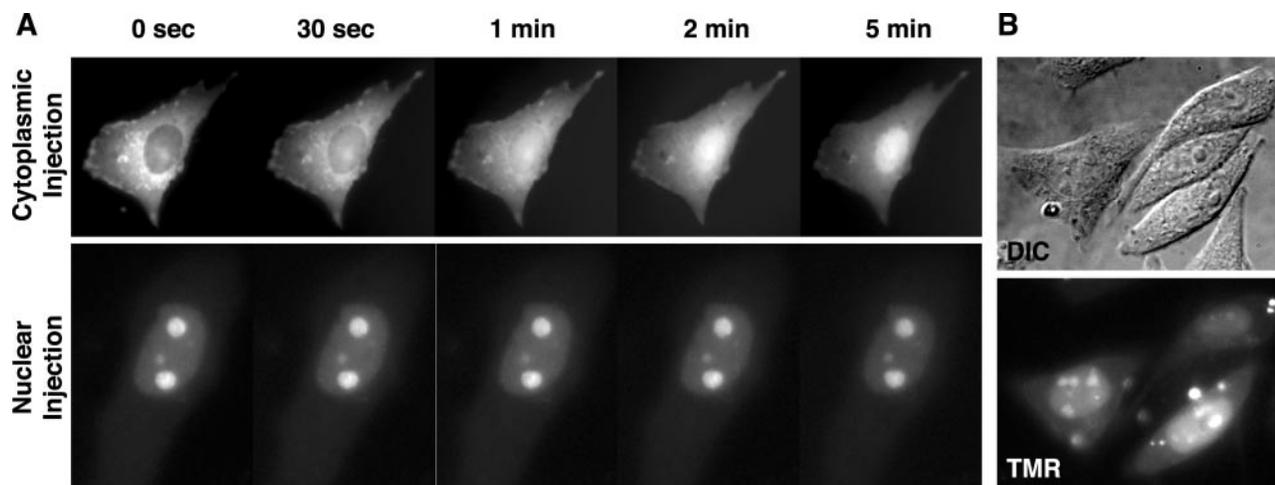
Figure 1. Sequestration of a molecular beacon analogue (that has no quencher and is designed not to bind to any RNA in the cell) into the nuclei of HeLa and CHO cells. (**A**) MB Analogue 1 (Table 1) was injected into the cytoplasm (top panel) or into the nucleus of HeLa cells (bottom panel) and its intracellular distribution was imaged as a function of time. The brighter spots within the nucleus are nucleoli. (**B**) The intracellular distribution of MB Analogue 1 after its transfection into CHO cells.

The speed and extent of nuclear sequestration after microinjection leaves very little time for molecular beacons to find their mRNA targets and bind to them. Although this phenomenon helps in the imaging of nuclear RNAs, it is undesirable for the imaging of cytoplasmic mRNAs.

Export of a synthetic tRNA transcript from the nucleus to the cytoplasm

We reasoned that it should be possible to use tRNAs as carriers to reverse the nuclear sequestration of molecular beacons, because large amounts of different tRNA species are constitutively exported from the nucleus to the cytoplasm. Since it is convenient to utilize synthetic transcripts, we first explored whether an *in vitro* transcribed tRNA (which lacks the modified nucleosides that are characteristic of natural tRNAs) is efficiently exported from the nucleus.

In order to study the ability of HeLa cells to export synthetic tRNAs, we prepared a human valine tRNA transcript that was labeled with TMR at some of its uridine residues. We microinjected this transcript into the nuclei of HeLa cells. In order to be sure that the injections were nuclear and that the injected material did not leak due to a break in the nuclear envelope, we included a 75 kDa dextran that was labeled with fluorescein in the injection mixture. Dextrans are not actively exported by the nucleus and when they are larger than 40 kDa, they cannot passively diffuse through nuclear pores (27). The cell was imaged immediately after injection and 25 min after injection, in order to follow both the tRNA (TMR-labeled) and the dextran (fluorescein-labeled). The images in Figure 2A show that, while dextran remained in the nucleus, tRNA was exported into the cytoplasm within 25 min. This export was specific for tRNA, as a number of tRNA variants that were missing particular stem–loop structures were not exported (28). The tRNAs were expelled in all cells that survived injection. In addition, we observed that a single-stranded DNA of the same sequence as the tRNA was not exported.

We also injected a mixture of tRNA transcripts and dextran into the cytoplasm of cells, in order to study their fate. A field of such cells is shown in Figure 2B, in which the large cell on the right-hand side of the micrograph received a cytoplasmic injection, as indicated by the distribution of dextran. The injected tRNA transcripts remained within the cytoplasm for at least 40 min.

Immediately after injection within the nucleus, the tRNA transcript was concentrated in the nucleoli of the cells (see the middle image in the left panel of Figure 2A). This is consistent with the nucleoli being the normal site of tRNA synthesis and processing (29,30). Nucleolar staining faded as the tRNA transcripts were exported out of the nucleus. We also observed that soon after their export from the nucleus, the tRNA transcripts were relatively homogenously distributed in the cytoplasm, but with time they became clustered in the cytoplasm on one side of the nucleus. A similar change in the distribution of the tRNA transcripts was observed when they were injected directly into the cytoplasm (Figure 2B).

Export of a transcript containing both a molecular beacon sequence and a tRNA sequence

tRNAs are produced in the nucleus with extra sequences present at each of their ends, and some tRNA genes harbor introns. Several processing events occur that remove the extensions and the introns, add CCA to the 3′ end, and chemically modify some of the nucleotides to produce fully mature tRNAs, before they are exported to the cytoplasm (21). It is believed that the tRNA export machinery is highly discriminative and exports only mature tRNAs, leaving behind unprocessed or partially processed tRNAs (31). Given the reported high fidelity of the tRNA export system, we decided to study the export of tRNA transcripts possessing a molecular beacon sequence at their 5′ end. RNA transcripts containing both a molecular beacon sequence and a tRNA sequence [MB-poly(U)-tRNA, Table 1] and labeled internally with TMR (Figure 3A) were injected into HeLa cells along with fluorescein-labeled dextran. After a 30-min incubation, the cells were imaged (Figure 3B). The cells that received a nuclear injection exported the molecular beacon–tRNA transcripts
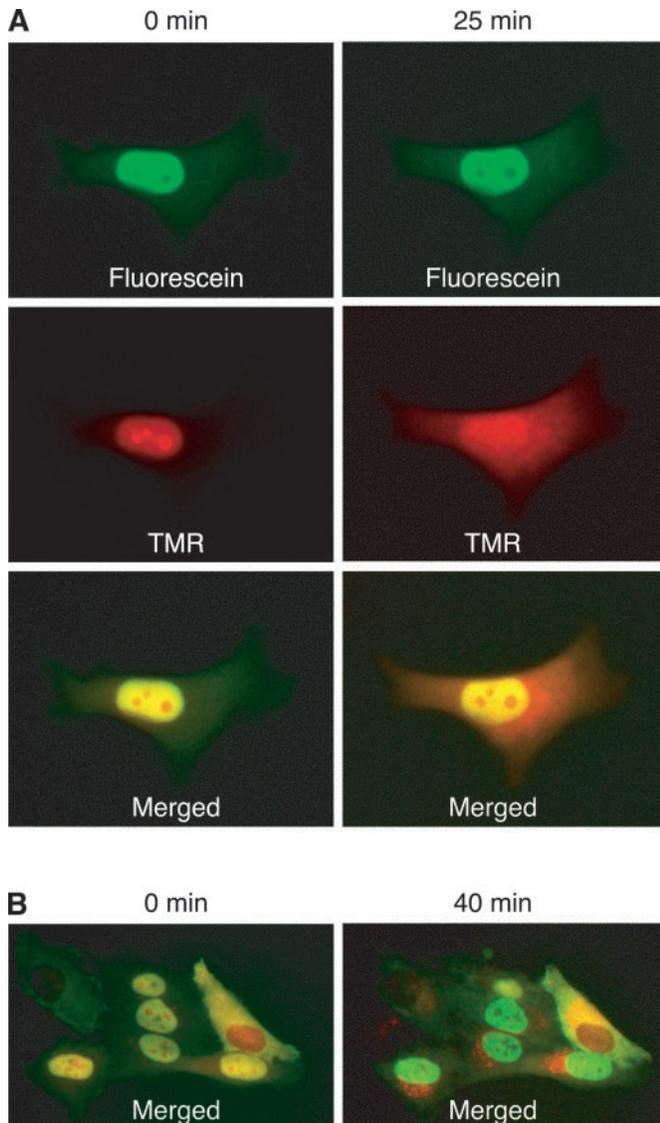
Figure 2. Intracellular distribution of fluorescently labeled tRNA[val] transcripts after injection. tRNA labeled with TMR (red) and 75 kDa dextran (that cannot traverse nuclear pores) labeled with fluorescein (green) were co-injected into HeLa cells. (**A**) Component and composite images of a cell that received a nuclear injection. (**B**) Composite images of a field of cells which includes two cells that received a cytoplasmic injection.

from the nucleus to the cytoplasm, whereas cells injected cytoplasmically with these transcripts retained them in the cytoplasm.

It can be argued that the tRNA processing machinery was able to trim the molecular beacon sequence from the 5′ end of the tRNA sequence, and that the rest of the tRNA was exported. However, this is unlikely because the 5′ sequence in MB poly(U)-tRNA does not match the sequence that occurs at the 5′ end of the natural precursors of tRNAs. The 5′ leader sequence in the tRNA precursor must be recognized by the pre-tRNA processing enzyme RNase P for its removal (21). Nevertheless, we synthesized a version of MB poly(U)-tRNA that contained a single TMR label at its 5′ end and injected it into nuclei (Figure 3C). The appearance of the TMR label in the cytoplasm in this case would indicate the export of

full-length construct. Since this singly labeled transcript is much less fluorescent, and since dextran's fluorescence could obscure the fluorescence of the TMR label, we did not include dextran in the injection mixture. After injection, the distribution of the fluorescence of the singly labeled transcripts was followed as a function of time (Figure 3D). The results show that a substantial portion of the injected transcripts were exported into the cytoplasm and their distribution in the cytoplasm was similar to the distribution of the tRNA transcripts.

Export of 2′-*O*-methylribonucleotide molecular beacons covalently linked to tRNA transcripts and using them to image the distribution of the general mRNA population

Encouraged by these results, we developed a strategy to covalently link a tRNA transcript to a 2′-*O*-methylribonucleotide molecular beacon. In this strategy, we introduced a sulfhydryl group at the 5′ end of the tRNA transcript, and a primary amino group at the 3′ end of a 2′-*O*-methylribonucleotide molecular beacon. These two molecules were then linked to each other using a heterobifunctional agent. A schematic representation of this chimeric construction [MB poly(U)-linker-tRNA] is shown in Figure 4A and its sequence is shown in Table 1. The loop sequence of the molecular beacon in this construct was designed to recognize the poly(A) tails of the general mRNA population. The tRNA used in this construct was not labeled with any fluorophore. In preliminary experiments, we determined that the linkage of the tRNA sequence to the molecular beacon sequence did not substantially affect the ability of the molecular beacon sequence to spontaneously bind to its target and produce a fluorogenic response.

Figure 4B shows that MB poly(U)-linker-tRNA, similar to unmodified tRNAs and their counterparts with 5′ extensions, is also exported from the nucleus to the cytoplasm. In order to image the cytoplasmic distribution of the general mRNA population, we injected MB poly(U)-linker-tRNA into the cytoplasm of HeLa cells and imaged a central plane of the injected cells as a function of time. Figure 4C shows a confocal image that was acquired 3 h after injection. It shows that there was no accumulation of fluorescence in the nucleus and that all of the probes were retained in the cytoplasm. Fluorescence in the cytoplasm was distributed in the punctate pattern that is characteristic of the distribution of poly(A) mRNA in the cytoplasm (32,33), confirming successful hybridization of MB poly(U)-linker-tRNA with the poly(A) tails of the mRNAs.

Linking molecular beacons to tRNA via engineered cohesive ends

The concentrations of the probes and the targets and the conditions inside the cell are such that it takes only 15–30 min to substantially complete hybridization (10,16). It might therefore be possible to retain the probes in the cytoplasm for these lengths of time by linking the probe to the tRNA transcript non-covalently. To explore this idea, we designed tRNA transcripts and molecular beacons that contained complementary overhanging sequences at their 3′ ends, so that they could bind to each other (Figure 5A). We chose a 15-nt-long sequence with a high-GC-content for the cohesive ends, in order to create a firm link (Table 1).
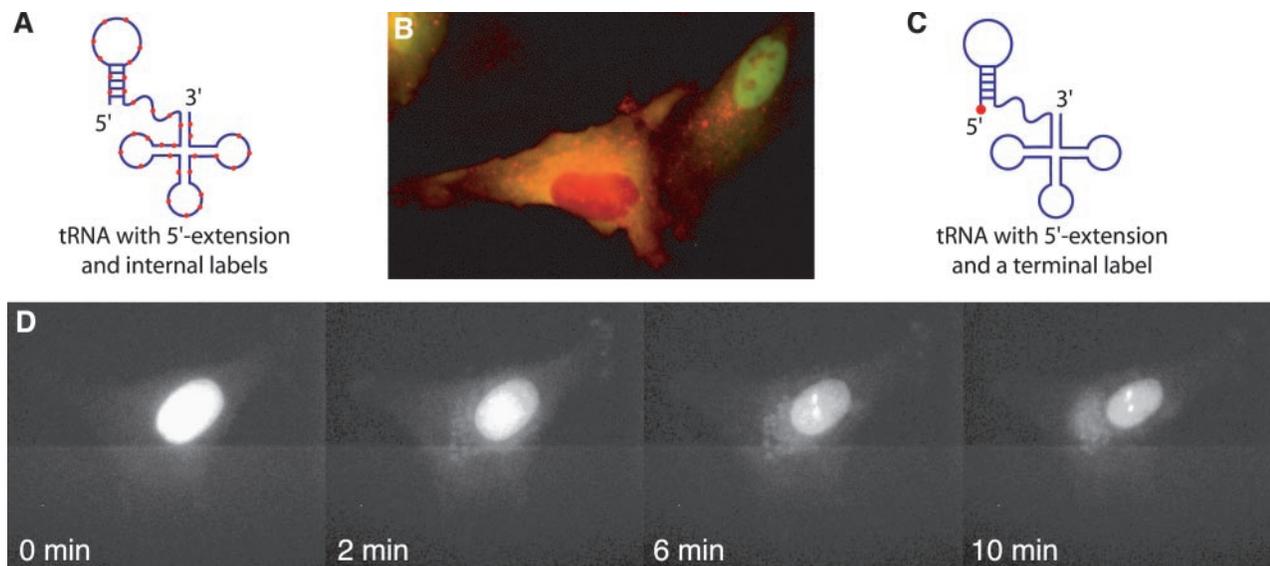
Figure 3. Export of RNAs containing a molecular beacon sequence and a tRNA sequence in the same transcript [MB poly(U)-tRNA, Table 1]. (**A**) Schematic representation of MB poly(U)-tRNA internally labeled with TMR. (**B**) Composite image of two cells 30 min after injection of TMR-labeled poly(A)-tRNA and fluorescein-labeled dextran. The cell on the right received a nuclear injection and the cell on the left received a cytoplasmic injection. The red color represents TMR fluorescence and the green color represents fluorescein fluorescence. (**C**) Schematic representation of MB poly(U)-tRNA labeled with a single TMR moiety at its 5′ end. (**D**) Monitoring the export of terminally labeled MB poly(U)-tRNA from the nucleus to the cytoplasm as a function of time after nuclear injection.
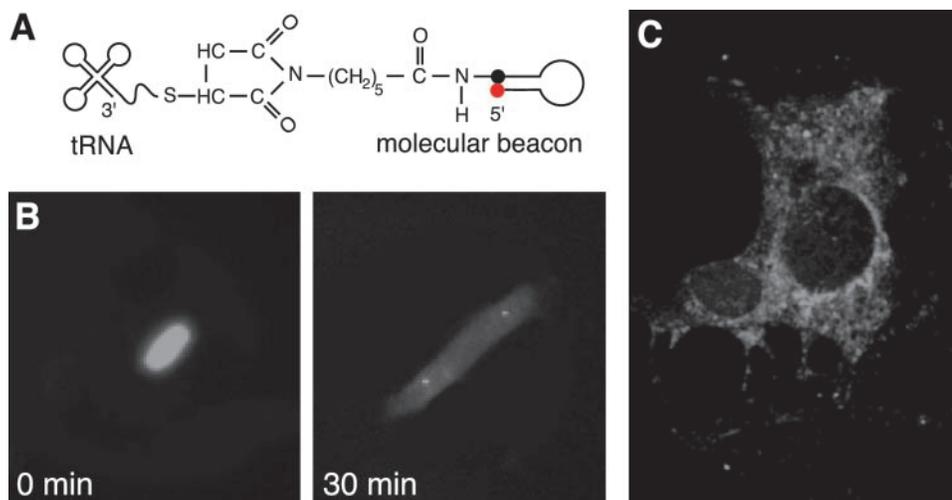

Figure 4. Export of molecular beacons covalently linked to tRNA transcripts. (**A**) Schematic representation of a tRNA conjugated with a molecular beacon [MB poly(U)-linker-tRNA, Table 1]. The linker that is shown is introduced when the heterobifunctional coupling agent mal-sac-HNSA is used to link a tRNA transcript with a 5′-sulfydryl group to a molecular beacon with a 3′-amino group. Black and red dots identify the quencher and the fluorophore of the molecular beacon. (**B**) Intracellular distribution of MB poly(U)-linker-tRNA immediately after and 30 min after nuclear injection. (**C**) Imaging the distribution of the general mRNA pool in the cytoplasm. MB poly(U)-linker-tRNA was injected into the cytoplasm of a HeLa cell and a confocal image from a central plane was acquired 3 h later.

In order to determine if the bond between the cohesive ends of the tRNA transcripts and the molecular beacons is strong enough to keep the molecular beacons within the cytoplasm, we utilized a second 'quencher-less' molecular beacon analogue (MB Analogue 2, Table 1). Two versions of this analogue were prepared. The first version was labeled with TMR and the second was labeled with Texas red. The TMR-labeled preparation of MB Analogue 2 was annealed to a tRNA transcript possessing a complementary overhang (tRNA Sticky End, Table 1) and was then purified via non-denaturing gel electrophoresis. This TMR-labeled complex and the Texas red-labeled free MB Analogue 2 were co-injected into the cytoplasm of a CHO cell. Figure 5B shows that the free MB Analogue 2 became sequestered within the nucleus, whereas the molecular beacon bound to the tRNA transcript remained largely cytoplasmic. A detectable fraction of tRNA-linked analogue was also able to enter the nucleus (as indicated by the staining of the nucleoli) perhaps due to the dissociation of the cohesive ends. This pattern was observed in all cells that were injected, some of which are displayed in Figure 5C.
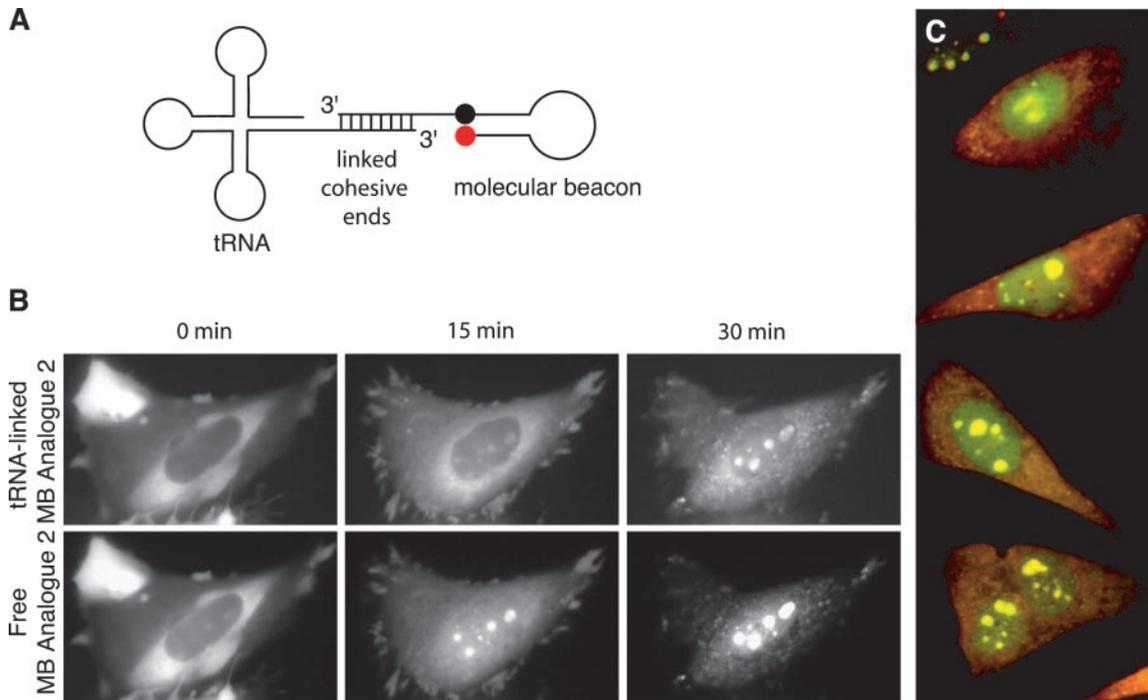
Figure 5. Cytoplasmic retention of a molecular beacon linked to a tRNA via engineered cohesive ends. (**A**) Schematic representation of the complex formed between a tRNA transcript and a molecular beacon through complementary sequences introduced at their respective 3′ ends. The red dot at the 5′ end of the molecular beacon identifies the fluorophore and the black dot represents the internal quencher moiety. (**B**) Cytoplasmic retention of MB Analogue 2 when it is linked to tRNA and its nuclear sequestration when it is not linked to tRNA. A mixture containing TMR-labeled MB Analogue 2 linked with tRNA and a Texas red-labeled MB Analogue 2 that was not linked to tRNA was injected into the cytoplasm of CHO cells. Changes in the distribution of each form of MB Analogue 2 were monitored by imaging the cell with respect to both TMR and Texas red. (**C**) Merged images of a set of representative cells after 30 min of incubation in which the fluorescence of MB Analogue 2 linked to tRNA is shown in red and the fluorescence of free MB Analogue 2 is shown in green.

Imaging the distribution of a specific mRNA

In order to explore the suitability of this approach for imaging specific cytoplasmic mRNAs, we selected as target the mRNA that encodes β-actin in chicken embryonic fibroblasts. This mRNA is concentrated in cytoplasmic regions that are proximal to the leading edges of the lamellipodia, which are protrusions that cells extend to enable them to adhere to surface as they move (34). This system was selected because a unique and characteristic distribution of fluorescence signals results from the localized mRNA, the β-actin mRNA is highly abundant and thus produces strong signals, and we have previously identified several molecular beacon sequences that bind well to β-actin mRNA (16).

In order to obtain strong fluorescence signals, we simultaneously utilized three molecular beacons that each bind to β-actin mRNA at different sites. Each of these molecular beacons had a single-stranded overhanging sequence at their 3′ end (Table 1). This sequence was complementary to a 3′ overhang sequence in the tRNA transcript tRNA Sticky End (Table 1). Two versions of these probes were prepared. The first version was labeled with TMR and the second was labeled with Texas red. The Texas red-labeled preparations of the β-actin mRNA-specific molecular beacons were annealed to tRNA Sticky End transcripts and the complexes were then purified via non-denaturing gel electrophoresis.

Since it is possible that the attached tRNA would adversely affect the ability of the probes to bind to their target sequences and might interfere with the quenching of the fluorophore, we first measured the kinetics of hybridization of free molecular beacons to full-length β-actin mRNA transcripts, and compared those results with the kinetics of hybridization of molecular beacons linked to tRNAs as they bound to full-length β-actin mRNA transcripts. The results of these comparisons are shown in Figure 6A. Each molecular beacon hybridized to the β-actin mRNA with its own characteristic speed, which decreased when the tRNA was attached. The magnitude of this decrease was different for each molecular beacon and probably reflected the contextual differences in the three target sites within the β-actin mRNA. The extent of quenching of the fluorophore, as indicated by the levels of fluorescence of molecular beacons before the addition of target, did not change appreciably.

After demonstrating that the linkage of tRNAs to molecular beacons does not substantially impair the ability of the molecular beacons to bind to mRNA *in vitro*, we used these linked constructs to image the distribution of β-actin mRNA in live chicken embryonic fibroblasts. We introduced a mixture of the three tRNA–linked molecular beacons into the cytoplasm of these cells. As a control designed to demonstrate the utility of tRNA attachment, we also included in this mixture a set of the same molecular beacons not linked to tRNA. The molecular beacons linked to tRNA were labeled with Texas red, whereas the free molecular beacons were labeled with TMR. The fibroblasts were imaged with respect to each label after 1 h of incubation at 37°C. The results show that most of the free molecular beacons were sequestered in the nucleus, whereas most of the tRNA–linked molecular beacons
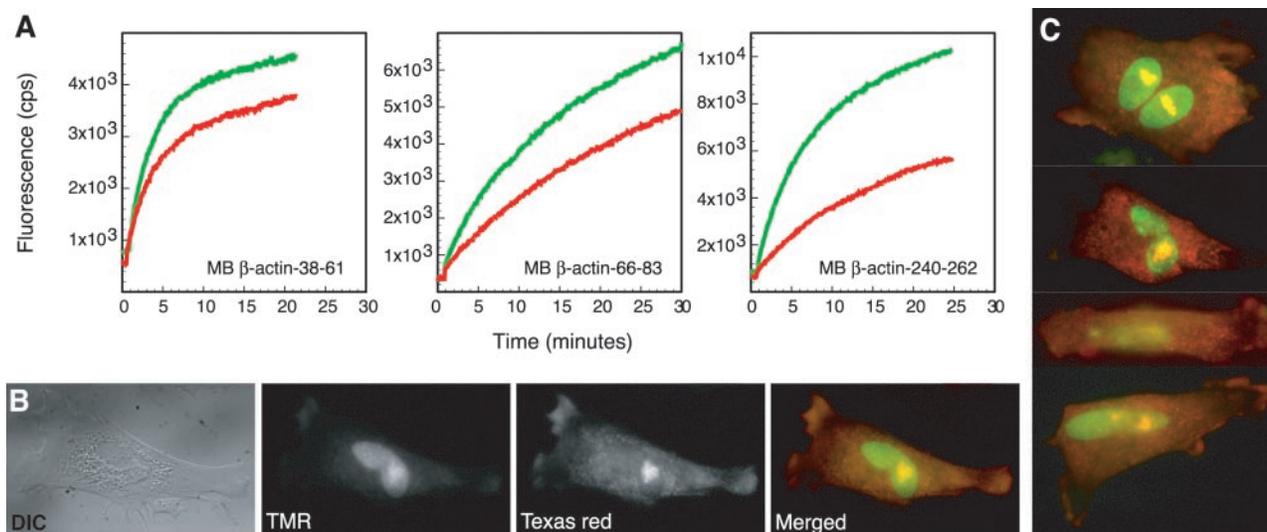
Figure 6. Detecting β-actin mRNA using molecular beacons linked to tRNA via sticky ends. (**A**) Effect of the attachment of tRNA on the kinetics of hybridization between different molecular beacons and full-length β-actin mRNA. The green curves show the results obtained from the real-time monitoring of hybridization reactions performed with molecular beacons that are not linked to tRNA, and red curves show the results obtained from the real-time monitoring of hybridization reactions containing the same molecular beacons linked to tRNA. (**B**) Imaging the distribution of β-actin mRNA in chicken embryonic fibroblasts using Texas red-labeled molecular beacons linked to tRNA and TMR-labeled free molecular beacons. The cells were imaged with respect to each fluorophore 1 h after cytoplasmic injection of the mixture of probes. (**C**) Merged images of cells that remained mobile. The red color represents the fluorescence of the tRNA-linked molecular beacons and the green color represents the fluorescence of molecular beacons not linked to tRNA.

remained in the cytoplasm (Figure 6B). The cytoplasmic molecular beacons were able to bind to the β-actin mRNA as indicated by the fluorescence seen in the active lamellipodia of the cells (Figure 6B). A similar distribution of the fluorescence signals was seen in other cells that were moving actively (Figure 6C). These results are consistent with the distribution of β-actin mRNA that was previously observed by *in situ* hybridization (34). These results demonstrate that the presence of a tRNA transcript on the end of molecular beacons enables the molecular beacons to be retained in the cytoplasm, yet the tRNAs do not significantly interfere with the binding of the molecular beacons to their targets and the generation of target-specific fluorescence signals.

DISCUSSION

Initially, we hypothesized that there would be a dynamic equilibrium between the entry of the molecular beacon–tRNA conjugate into the nucleus and its export from the nucleus to the cytoplasm, with export being favored. However, we found that cytoplasmically injected tRNAs and their conjugates did not enter the nucleus to any significant extent. The cytoplasmic retention of these constructs may be due to the association of the tRNAs with elements of the protein synthesis system (35). Immediately after direct injection into the cytoplasm, or immediately after export from the nucleus, the tRNA was distributed relatively homogenously in the cytoplasm. However, after 30 min, it tended to concentrate on one side of the nucleus. This redistribution may reflect the distribution of proteins that are bound to tRNAs in the cytoplasm (35). This non-homogenous distribution of tRNA could have presented a problem for the imaging of mRNA distribution. However, the images of the distribution of the general mRNA

population and the distribution of β-actin mRNA show that this was not the case.

Even though it was not our primary motivation, the results shed light on the fidelity of tRNA export in mammalian cells. tRNA transcripts that were synthesized *in vitro*, which contained fluorophores at some of their uridine residues, and lacked modified nucleotides that are present in natural tRNAs, were exported from the nucleus. A 32-nt-long hairpin-shaped extension at their 5′ end did not prevent export. Furthermore, even when the extension had a 2′-*O*-methylribonucleotide backbone and was linked to tRNA via a non-phosphodiester spacer, export took place. Although these observations highlight the utility of these constructs for reversing the nuclear sequestration of molecular beacons, these observations run counter to the widely accepted view that only fully processed and mature tRNAs can be exported from the nucleus (31,36). However, these studies [and earlier studies (37,38)] point out that if excessive amounts of tRNA precursors are introduced into the nucleus, the tRNA precursors can be exported without processing. The amounts of transcript that we introduced could have overwhelmed the fidelity of the export system. The fidelity of tRNA export primarily depends upon the selectivity of exportin-t. Exportin-t is a receptor for tRNA that transports tRNAs through the nuclear pores of higher eukaryotes (39). Lipowsky *et al*. (40) have determined that the affinity of exportin-t for unmodified tRNAs and unmodified tRNAs possessing 5′-extensions, are 20 and 2.4%, respectively, relative to the affinity of exportin-t for fully processed tRNAs. This suggests that it is possible to export unnatural tRNAs and their variants when they are introduced into the nucleus in large amounts.

During the course of this work, we developed a simple method for specifically labeling RNAs at their 5′ end with fluorophores and other moieties. In this method, the 5′ label

is introduced by including a derivative of 5′-thio-GMP in the transcription mixture. Using these labels, it is simple to couple the RNA to an oligonucleotide containing a primary amino group. This approach can easily be adopted to link RNAs to proteins, dyes and other molecules.

In summary, we have shown that the nuclear sequestration of molecular beacons can be overcome by attaching them to *in vitro*-transcribed tRNAs. The presence of tRNAs on the molecular beacons increases the residence time of the molecular beacons in the cytoplasm and enables them to bind specifically to target mRNAs, signaling the presence of their targets. Previously, we linked bulky proteins to molecular beacons in order to stop their entry into the nucleus through the nuclear pores. A peptide corresponding to the nuclear export signal may similarly be useful in this regard. The advantage of using tRNA transcripts is that they offer a simple means of attachment via engineered cohesive ends. These approaches will also help to increase the effectiveness of antisense agents whose biological activity is hampered by nuclear sequestration.

REFERENCES

1. Tekotte,H. and Davis,I. (2002) Intracellular mRNA localization: motors move messages. *Trends Genet.*, **18**, 636–642.
2. Heller,M.J. and Morrison,L.E. (1985) Chemiluminescent and fluorescent probes for DNA hybridization systems. In Kingsbury,D.T. and Falkow,S. (eds), *Rapid Detection and Identification of Infectious Agents*. Academic Press, NY, pp. 345–356.
3. Cardullo,R.A., Agrawal,S., Flores,C., Zamecnik,P.C. and Wolf,D.E. (1988) Detection of nucleic acid hybridization by nonradiative fluorescence resonance energy transfer. *Proc. Natl Acad. Sci. USA*, **85**, 8790–8794.
4. Morrison,L.E., Halder,T.C. and Stols,L.M. (1989) Solution-phase detection of polynucleotides using interacting fluorescent labels and competitive hybridization. *Anal. Biochem.*, **183**, 231–244.
5. Tyagi,S. and Kramer,F.R. (1996) Molecular beacons: probes that fluoresce upon hybridization. *Nat. Biotechnol.*, **14**, 303–308.
6. Sixou,S., Szoka,F.C.,Jr, Green,G.A., Giusti,B., Zon,G. and Chin,D.J. (1994) Intracellular oligonucleotide hybridization detected by fluorescence resonance energy transfer (FRET). *Nucleic Acids Res.*, **22**, 662–668.
7. Tsuji,A., Koshimoto,H., Sato,Y., Hirano,M., Sei-Iida,Y., Kondo,S. and Ishibashi,K. (2000) Direct observation of specific messenger RNA in a single living cell under a fluorescence microscope. *Biophys. J.*, **78**, 3260–3274.
8. Matsuo,T. (1998) *In situ* visualization of mRNA for basic fibroblast growth factor in living cells. *Biochim. Biophys. Acta*, **1379**, 178–184.
9. Sokol,D.L., Zhang,X., Lu,P. and Gewirtz,A.M. (1998) Real time detection of DNA·RNA hybridization in living cells. *Proc. Natl Acad. Sci. USA*, **95**, 11538–11543.
10. Bratu,D.P., Cha,B.J., Mhlanga,M.M., Kramer,F.R. and Tyagi,S. (2003) Visualizing the distribution and transport of mRNAs in living cells. *Proc. Natl Acad. Sci. USA*, **100**, 13308–13313.
11. Leonetti,J.P., Mechti,N., Degols,G., Gagnor,C. and Lebleu,B. (1991) Intracellular distribution of microinjected antisense oligonucleotides. *Proc. Natl Acad. Sci. USA*, **88**, 2702–2706.
12. Lorenz,P., Misteli,T., Baker,B.F., Bennett,C.F. and Spector,D.L. (2000) Nucleocytoplasmic shuttling: a novel *in vivo* property of antisense phosphorothioate oligodeoxynucleotides. *Nucleic Acids Res.*, **28**, 582–592.
13. Beltinger,C., Saragovi,H.U., Smith,R.M., LeSauteur,L., Shah,N., DeDionisio,L., Christensen,L., Raible,A., Jarett,L. and Gewirtz,A.M. (1995) Binding, uptake, and intracellular trafficking of phosphorothioate-modified oligodeoxynucleotides. *J. Clin. Invest.*, **95**, 1814–1823.
14. Mathew,E., Hardee,G.E., Bennett,C.F. and Lee,K.D. (2003) Cytosolic delivery of antisense oligonucleotides by listeriolysin O-containing liposomes. *Gene Ther.*, **10**, 1105–1115.
15. Spiller,D.G., Giles,R.V., Grzybowski,J., Tidd,D.M. and Clark,R.E. (1998) Improving the intracellular delivery and molecular efficacy of antisense oligonucleotides in chronic myeloid leukemia cells: a comparison of streptolysin-O permeabilization, electroporation, and lipophilic conjugation. *Blood*, **91**, 4738–4746.
16. Tyagi,S. and Alsmadi,O. (2004) Imaging native β-actin mRNA in motile fibroblasts. *Biophys. J.*, **87**, 4153–4162.
17. Santangelo,P.J., Nix,B., Tsourkas,A. and Bao,G. (2004) Dual FRET molecular beacons for mRNA detection in living cells. *Nucleic Acids Res.*, **32**, e57.
18. Nitin,N., Santangelo,P.J., Kim,G., Nie,S. and Bao,G. (2004) Peptide-linked molecular beacons for efficient delivery and rapid mRNA detection in living cells. *Nucleic Acids Res.*, **32**, e58.
19. Gallouzi,I.E. and Steitz,J.A. (2001) Delineation of mRNA export pathways by the use of cell-permeable peptides. *Science*, **294**, 1895–1901.
20. Pasquinelli,A.E., Ernst,R.K., Lund,E., Grimm,C., Zapp,M.L., Rekosh,D., Hammarskjold,M.L. and Dahlberg,J.E. (1997) The constitutive transport element (CTE) of Mason–Pfizer monkey virus (MPMV) accesses a cellular mRNA export pathway. *EMBO J.*, **16**, 7500–7510.
21. Wolin,S.L. and Matera,A.G. (1999) The trials and travels of tRNA. *Genes Dev.*, **13**, 1–10.
22. Kuwabara,T., Warashina,M., Koseki,S., Sano,M., Ohkawa,J., Nakayama,K. and Taira,K. (2001) Significantly higher activity of a cytoplasmic hammerhead ribozyme than a corresponding nuclear counterpart: engineered tRNAs with an extended 3′ end can be exported efficiently and specifically to the cytoplasm in mammalian cells. *Nucleic Acids Res.*, **29**, 2780–2788.
23. Tyagi,S., Bratu,D.P. and Kramer,F.R. (1998) Multicolor molecular beacons for allele discrimination. *Nat. Biotechnol.*, **16**, 49–53.
24. Tyagi,S., Landegren,U., Tazi,M., Lizardi,P.M. and Kramer,F.R. (1996) Extremely sensitive, background-free gene detection using binary probes and beta replicase. *Proc. Natl Acad. Sci. USA*, **93**, 5395–5400.
25. Aldwin,L. and Nitecki,D.E. (1987) A water-soluble, monitorable peptide and protein crosslinking agent. *Anal. Biochem.*, **164**, 494–501.
26. Hartig,R., Shoeman,R.L., Janetzko,A., Grub,S. and Traub,P. (1998) Active nuclear import of single-stranded oligonucleotides and their complexes with non-karyophilic macromolecules. *Biol. Cell*, **90**, 407–426.
27. Ribbeck,K. and Gorlich,D. (2001) Kinetic analysis of translocation through nuclear pore complexes. *EMBO J.*, **20**, 1320–1330.
28. Mhlanga,M.M. (2003) Utilizing nuclear cytoplasmic export pathways for the imaging of gene expression. Ph.D. Thesis, New York University, NY.
29. Thompson,M., Haeusler,R.A., Good,P.D. and Engelke,D.R. (2003) Nucleolar clustering of dispersed tRNA genes. *Science*, **302**, 1399–1401.
30. Bertrand,E., Houser-Scott,F., Kendall,A., Singer,R.H. and Engelke,D.R. (1998) Nucleolar localization of early tRNA processing. *Genes Dev.*, **12**, 2463–2468.
31. Simos,G. and Hurt,E. (1999) Transfer RNA biogenesis: a visa to leave the nucleus. *Curr. Biol.*, **9**, R238–R241.
32. Taneja,K.L., Lifshitz,L.M., Fay,F.S. and Singer,R.H. (1992) Poly(A) RNA codistribution with microfilaments: evaluation by *in situ* hybridization and quantitative digital imaging microscopy. *J. Cell Biol.*, **119**, 1245–1260.
33. Enninga,J., Levy,D.E., Blobel,G. and Fontoura,B.M. (2002) Role of nucleoporin induction in releasing an mRNA nuclear export block. *Science*, **295**, 1523–1525.
34. Lawrence,J.B. and Singer,R.H. (1986) Intracellular localization of messenger RNAs for cytoskeletal proteins. *Cell*, **45**, 407–415.

35. Stapulionis,R. and Deutscher,M.P. (1995) A channeled tRNA cycle during mammalian protein synthesis. *Proc. Natl Acad. Sci. USA*, **92**, 7158–7161.

36. Lund,E. and Dahlberg,J.E. (1998) Proofreading and aminoacylation of tRNAs before export from the nucleus. *Science*, **282**, 2082–2085.

37. Melton,D.A., De Robertis,E.M. and Cortese,R. (1980) Order and intracellular location of the events involved in the maturation of a spliced tRNA. *Nature*, **284**, 143–148.

38. Melton,D.A., Cortese,R., de Robertis,E.M., Trendelenburg,M.F. and Gurdon,J.B. (1980) Gene injection into amphibian oocytes. *Results Probl. Cell Differ.*, **11**, 8–14.

39. Arts,G.J., Fornerod,M. and Mattaj,I.W. (1998) Identification of a nuclear export receptor for tRNA. *Curr. Biol.*, **8**, 305–314.

40. Lipowsky,G., Bischoff,F.R., Izaurralde,E., Kutay,U., Schafer,S., Gross,H.J., Beier,H. and Gorlich,D. (1999) Coordination of tRNA nuclear export with processing of tRNA. *RNA*, **5**, 539–549.